A Co-Polarized Microwave Absorber with Dual Mode Resonance Based on Dual Split Ring Geometry for Wi-Max and WLAN Applications

Gobinda Sen[1, *], Anumoy Ghosh[2], Mukesh Kumar[1], Sk. Nurul Islam[1], and Santanu Das[1]

Abstract—In this work, a dual-band microwave absorber is proposed with a periodic array of unit cells which has dual-split ring geometry on the top of a metal-backed dielectric substrate. The dual-split ring resonator on the top plane is electrically excited by the co-polarized component of incident EM wave and gives two absorption peaks at Wi-MAX (3.5 GHz) and WLAN (5.8 GHz) band due to two resonance modes. These two-resonance modes are named as mode 1 and mode 2 for low and high frequency peaks, respectively. The surface current distributions on the top and bottom planes are studied to gain insight into dual-mode resonance for dual-band absorption of the structure. Some parametric studies are also performed on key design parameters, i.e., split gap, stub length, and split angle for further analysis of the design. The measured results are verified with the simulated ones to test their performance and found to be similar.

1. INTRODUCTION

In the design of microwave absorbers, metamaterials have a potential application due to ultra-thin configuration, compact size, and near perfect absorption. Since the proposal of the first metamaterial perfect absorber by Landy et al. [1], a rapid evolution has come in the design of metamaterial absorber. A periodic array of split-ring-resonators (SRRs) are used [1, 2] to realize a metamaterial absorber for perfect absorption. At resonant frequency, the coupling of an incident electromagnetic field with SRRs [3] provides negative permittivity and permeability, and hence its electromagnetic properties can be artificially manipulated by tailoring element dimensions [4]. Over the years, several works on the design of a microwave absorber with polarization insensitive performance [5–7], wide incident angle operation [8–11], and multi-band absorption [5, 9, 10, 12] have been achieved.

With the growing demand for wireless access for wireless communication, Worldwide Interoperability for Microwave Access (Wi-Max) and Wireless LAN (WLAN) frequency bands has found potential applications. The widespread use of wireless communication at those frequency bands increases electromagnetic interference (EMI) in the electronics equipment. This leads to researchers' potential interest to develop some types of absorbing materials to reduce electromagnetic hazards at those bands.

Electric and Magnetic Resonances in SRRs: Different orientations of SRRs along with field components E and H of incident EM wave and wave vector k are given in Fig. 1. The induced surface currents on SRR due to incident field E^i satisfy the following boundary condition [4] on its surfaces as,

$$n(r) \times \left[E^s(r) + E^i(r)\right] = Z(r)\left[n(r) \times J(r)\right] \tag{1}$$
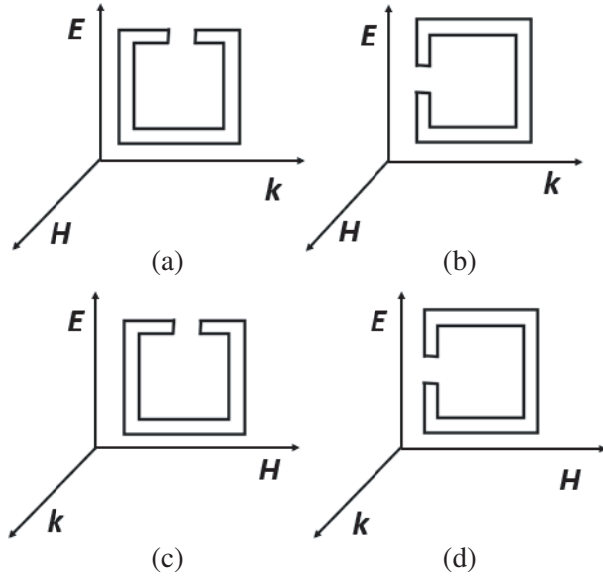
Figure 1. SRR geometry and their orientation with respect to the k, E and H vector of the incident wave.
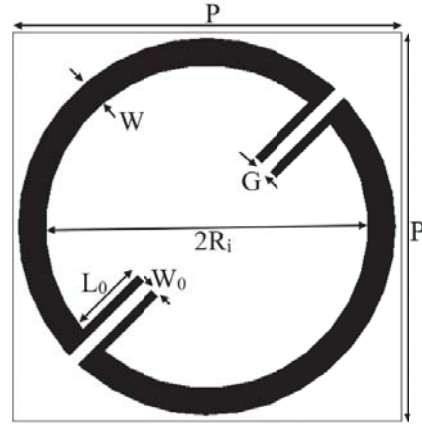
Figure 2. Unit cell of the proposed SRR based dual-band absorber.

where $n(r)$ is the normal vector to conductor surface; $E^s(r)$ is scattered electric field component due to induced current; and $Z(r)$ is the surface impedance of the SRR structure. In these orientations, magnetic resonance occurs when incident magnetic field (H) is perpendicular, and wave vector (k) is parallel to SRR plane [3] as in Figs. 1(a)–(b). A strong magnetic resonance occurs in both cases due to the large current induced on the SRR surface. In two other orientations as in Figs. 1(c)–(d), where H is parallel to the SRR plane, and no coupling of the incident field due to magnetic resonance occurs. However, if the electric field (E) is parallel to the gap bearing side of SRR (in Fig. 1(d)), a magnetic resonance occurs due to the electric coupling of the incident wave. Hence, the incident electric field excites the resonant oscillation of circular current inside SRR.

In this work, a dual-band microwave absorber is proposed with a periodic array of unit cells comprising dual-split ring geometry on top of a metal-backed dielectric substrate. This structure gives two absorption peaks at Wi-MAX (3.5 GHz) and WLAN (5.8 GHz) bands due to two resonance modes. These two-resonance modes are named as mode 1 and mode 2 for low and high frequency absorption peaks, respectively. The surface impedance of the proposed design is matched with free space resulting in no reflection of an incident wave at those dual absorption peaks.

2. DESIGN OF DUAL-SPLIT RING ABSORBER

The absorbed power in electromagnetic absorber can be represented from fundamental formulae as

$$A(\omega) = 1 - R(\omega) - T(\omega) \tag{2}$$

where $R(\omega)$ and $T(\omega)$ are reflection and transmission of the absorbing structure. The metal-backed substrate ensures the transmission to be zero; therefore, Equation (2) is modified as

$$A(\omega) = 1 - R(\omega) \tag{3}$$

$$A(\omega) = 1 - |S_{11}|^2 \tag{4}$$

where S_{11} is a reflection coefficient at the boundary. Therefore, to maximize absorption, the reflection coefficient is to be minimized as depicted from the equations. The effective normalized input impedance of the structure can be represented in terms of S-parameters as,

$$Z_{eff.}(\omega) = \sqrt{\frac{(1 + S_{11})^2 - S_{21}^2}{(1 - S_{11})^2 - S_{21}^2}} \tag{5}$$

The completely metallic back plane ensures transmission, and S_{21} is zero. Hence, Equation (5) can be rewritten as,

$$Z_{eff.}(\omega) = \sqrt{\frac{(1+S_{11})^2}{(1-S_{11})^2}} \tag{6}$$

The goal of the presented work is to obtain dual-band absorption at Wi-Max and WLAN frequency bands with the help of compact single unit cell resonator. A dual-split ring geometry as given in Fig. 2 is chosen for the design of the unit cell of the proposed absorber. The substrate is chosen as FR4-Epoxy of dielectric constant 4.4, and thickness is 2 mm. The electric field component of the incident EM wave induces two resonance modes at the split ring resonator (SRR). For convenience, these two modes are attributed as mode 1 and mode 2, where mode 1 and mode 2 are for lower and upper absorption peaks, respectively. The simulated dimensions are chosen for the operation of the proposed absorber for 3.5 GHz and 5.8 GHz applications. The values of design parameters are provided in Table 1.

Table 1. All dimensions in 'mm'.

P	W	R_i	W_0	L_0	G	h
13	0.9	5.4	0.3	2.58	0.4	2

3. SIMULATION RESULTS

The simulation and surface current distributions analysis of the proposed absorber (in Fig. 2) are obtained with CST Microwave Studio using unit-cell boundary conditions. A compact dual-split ring resonator structure gives dual-band absorption peaks at two important wireless application bands of 3.5 GHz and 5.8 GHz for both transverse electric (TE) and transverse magnetic (TM) polarizations under normal incident angles ($\theta = 0°$) as given in Fig. 3(a). Relative Absorption Bandwidths (RABs) of 1.44% and 3.60% are obtained at those absorption bands, respectively as calculated from that figure. The extracted normalized effective input impedance of the structure is obtained by calculation from Equation (6) as given in Fig. 3(b). The real and imaginary parts of that effective impedance are close to unity and zero, respectively at the absorption peaks of 3.5 GHz and 5.8 GHz. The absorption occurs at those frequencies due to the matching of the effective input impedance of the structure with free space.

Surface Current Distribution Analysis: The surface current distributions on the top (left) and bottom (right) planes at the dual absorption peaks of 3.5 GHz and 5.8 GHz are analysed to elaborate the absorption phenomena physically and given in Figs. 4(a)–(b) and (c)–(d), respectively. The distribution

(a)   (b)
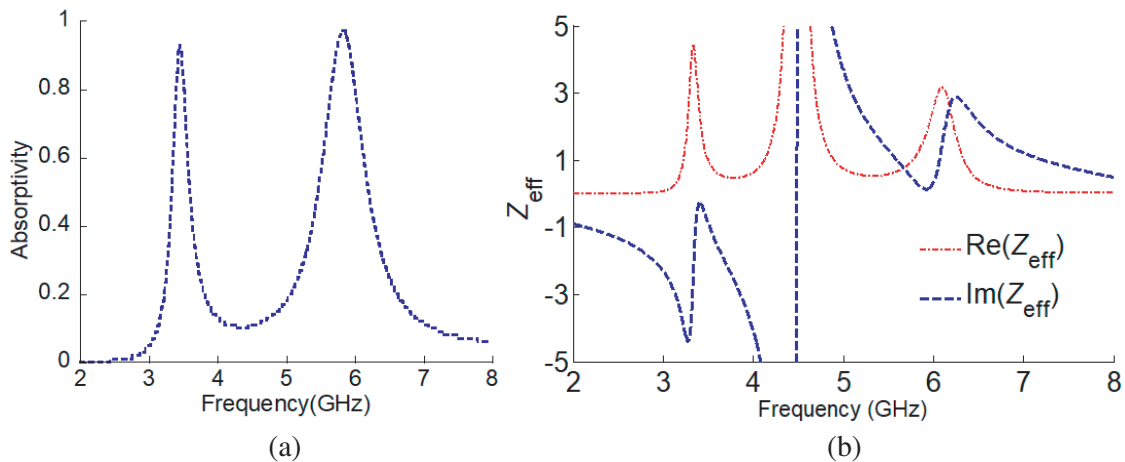
Figure 3. The proposed absorbers, (a) absorption performance at normal incidence for TE ($\phi = 0°$)/TM ($\phi = 90°$) mode, (b) effective normalized impedance plot.
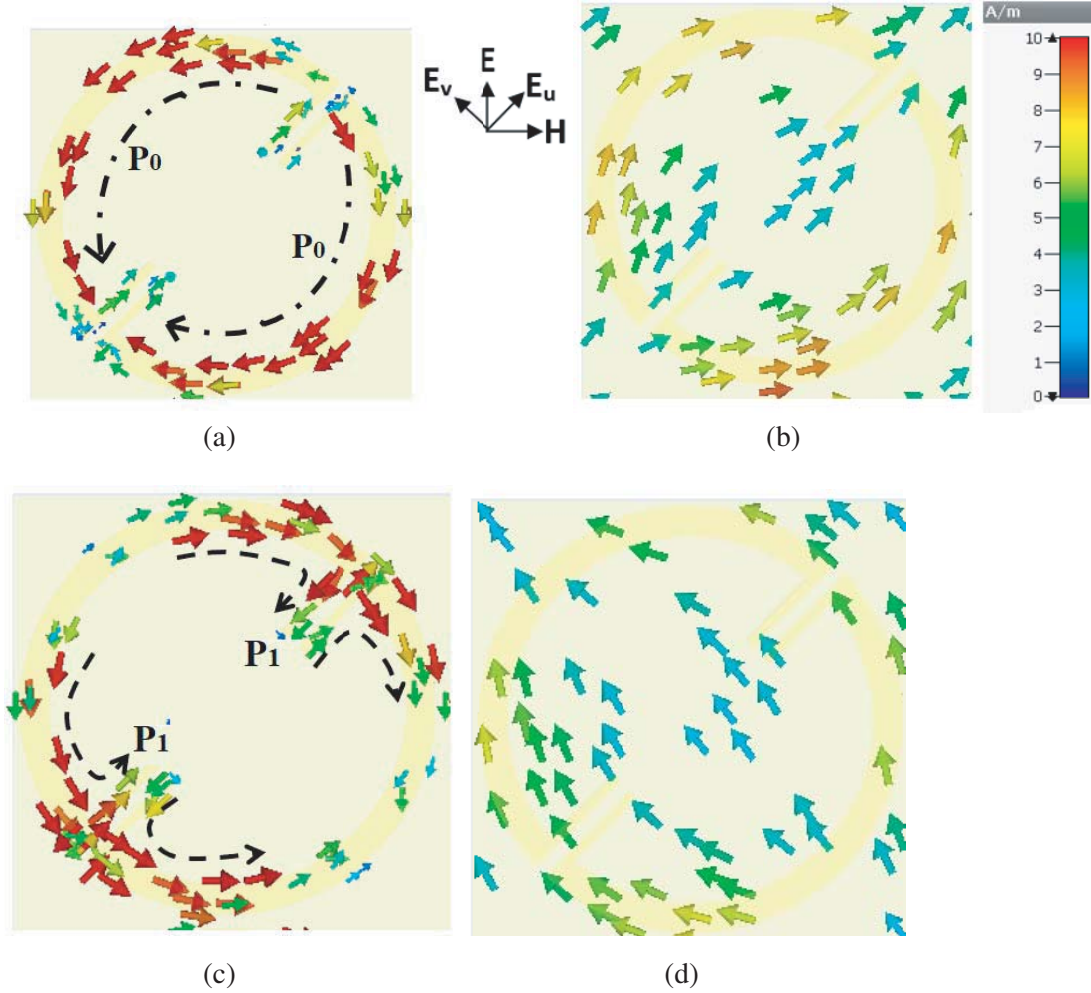
Figure 4. Surface current distribution on the top (left) and bottom planes (right) at (a)–(b) 3.5 GHz and (c)–(d) 5.8 GHz.

of surface currents on the top plane at the lower frequency of 3.5 GHz follows the half circular path (P_0) and is due to mode 1 resonance. The current vectors are primarily oriented along with the E_v component of the incident E field as observed from Figs. 4(a)–(b). A circulating current loop is formed due to the anti-parallel direction of currents in-between top and bottom metallic layers as depicted in the above figure. However, at the higher absorption peak of 5.8 GHz, the current vectors on the top and bottom planes of the proposed design (Fig. 2) are oriented mainly along with the E_u component of the incident E field and follow a path (P_1) as observed from Figs. 4(c)–(d). This is due to mode 2 resonance of the SRR structure. The path length (P_1) in mode 2 resonance is smaller than mode 1 resonance (P_0), and hence absorption peak is at higher frequency than mode 1 case. An anti-parallel surface current distribution in between top and ground planes is also observed at this frequency (5.8 GHz) which is due to the magnetic response of the structure. Hence both the electric and magnetic resonances contribute to the power loss within the structure.

Some Parametric Studies on Absorption Performances: Figs. 5(a)–(b) show the absorption performance of the structure with different polarization angles (ϕ) and incident angles (θ). The response of the structure is found to be the same for TE ($\phi = 0°$) and TM ($\phi = 90°$) modes of the incidence of an incoming EM wave and depicted in Fig. 5(a), whereas the absorption performance of the design for the polarization angle ϕ of 30° and 60° gives single band absorption due to mode 1 resonance, where surface current path is P_0 least affected by different values of ϕ. The dual-band absorption performance of structure (Fig. 2) is analysed for different values of incident angle (θ) as in Fig. 5(b). This result shows

that the first absorption peak at 3.5 GHz is consistent for all the values of θ due to mode 1 resonance, which follows the current path P_0. However at the higher frequency of 5.8 GHz, the performance is deteriorated due to surface current path P_1 along the split gap of the SRR structure.

Parametric studies on some of the design parameters like split gap (G), stub length (L_0), and Split angle (β) are conducted in Figs. 6(a), (b), and (c), respectively. The increase in 'G' results in the loose coupling between the semi-circular rings, and hence series capacitance decreases. The decrease in capacitance value results in an increase in resonance peak for mode 2, which follows the current path (P_1) along the split gap of the SRR structure as given in Fig. 6(a). However, for mode 1 resonance the lower absorption frequency peak is least bothered by G because split gap does not come inside of surface current path (P_0). The increase in stub length (L_0) causes an increase of inductance, and hence absorption frequency due to mode 2 resonance goes downward. However, the lower absorption peak at 3.5 GHz is not changed due to mode 1 resonance which is contributed by current path length (P_0) as in Fig. 6(b). Fig. 6(c) shows the change in split angle (β) from 0° to 45° result in the single band to dual-band absorption response because single mode to dual mode resonance occurs in the SRR structure. The orthogonal component of the electric field along the split axis is responsible for dual resonances in the structure for an angle $\beta = 45°$.
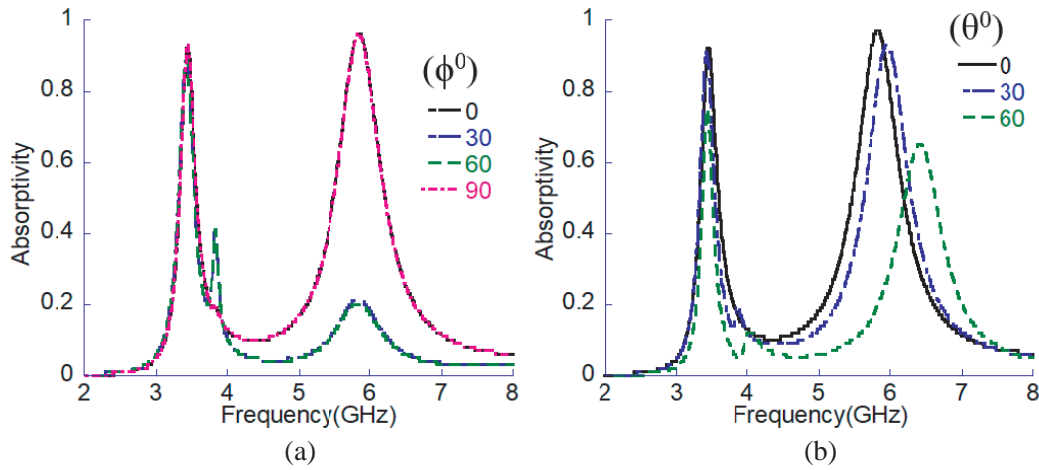
Figure 5. Absorption performance of the absorber with different (a) polarization angle (ϕ), (b) incident angle (θ).
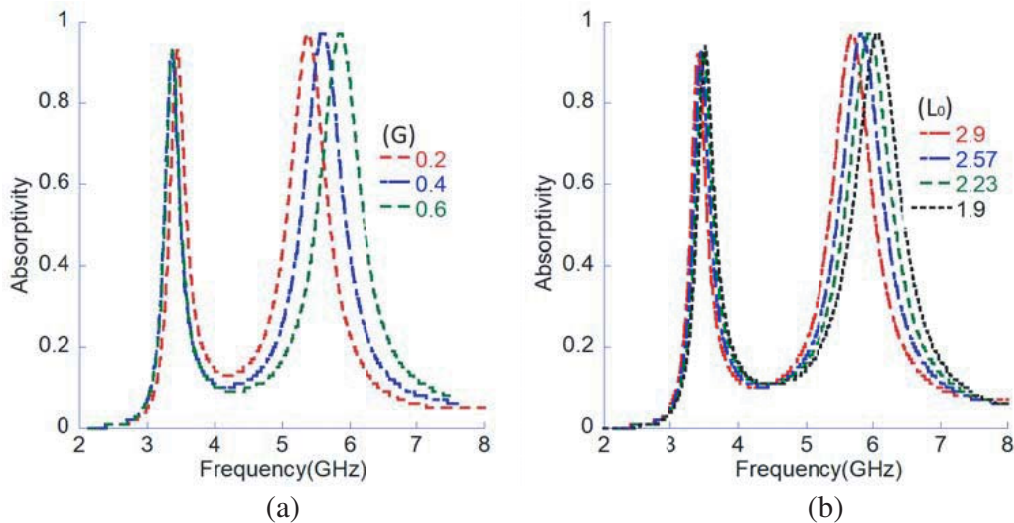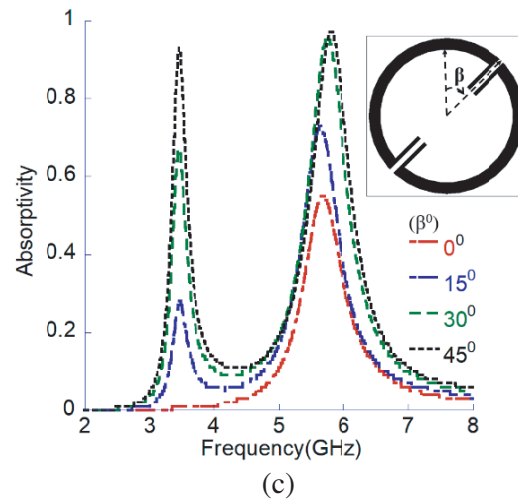
Figure 6. Parametric studies on the absorption performance with (a) split gap (G), (b) stub length (L_0) and (c) split angle (β).
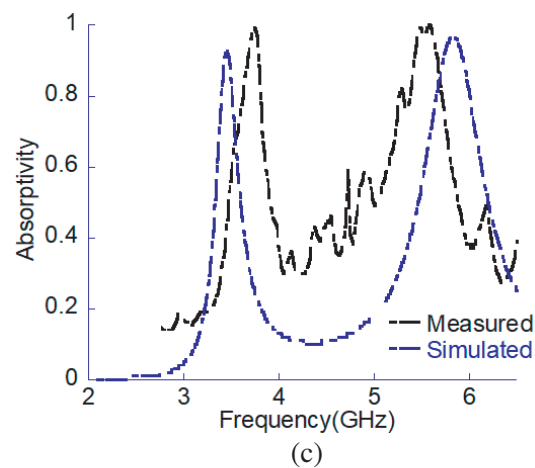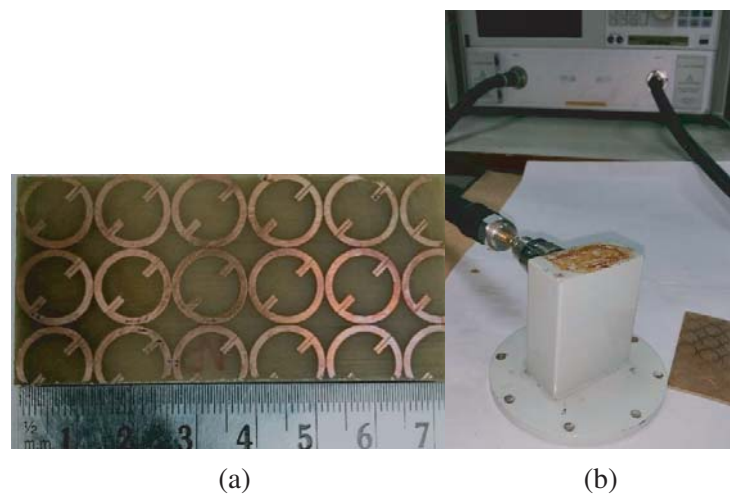
Figure 7. Fabricated prototype along with results, (a) structure, (b) setup, (c) measured and simulated results.

4. EXPERIMENTAL VALIDATION

A 4×3 array of unit cells of the proposed structure is fabricated as shown in Fig. 7(a). Fig. 7(b) depicts the waveguide measurement method [13–15] which is used to validate the design. An Agilent N5230A series Network Analyzer and two standard waveguides operate in the S-band and C-band are used for the measurement process. The electromagnetic wave comes out from the waveguide is incident at the interface of the sample at an oblique angle of $\theta = \sin^{-1}(\lambda/2a)$ ('a' is the width of the aperture, and λ is the wavelength). The oblique incident angles at the frequencies of 3.5 GHz and 5.8 GHz are calculated as $36°$ and $32°$, respectively. A good absorption performance over the proposed one is obtained at 3.75 GHz and 5.60 GHz with RABs of 3.76% and 4.50%, respectively, and given in Fig. 7(c). In Table 2, the novelty of this proposed dual-band absorber is validated by comparing it with some of the pre-existing dual-band microwave absorbers available in the literature. In [16], a dual-band absorber is proposed with a thin substrate of thickness 2.4 mm, but a larger unit cell dimension and complex structure limit its applicability. In [17, 18], dual-band absorbers are achieved with smaller cell area and substrate height than [16], but structural complexity also increases. The work presented here is proved to have advantages as compared to cell element, cell area, and substrate height for the application frequency.

Table 2. Comparison table.

Design	Unit Cell Area (mm^2)	Lowest Absorption Peak (GHz)	Thickness (mm)	Characteristics
[16]	27.4×27.4	1.92	2.4	Dual Band
[17]	19.9×19.9	4.32	1.6	Dual Band
[18]	18.4×18.4	5.95	0.8	Dual Band
This work	13×13	3.5	2	Dual Band

5. CONCLUSION

This work aims to provide dual-band absorption at Wi-MAX and WLAN frequencies with a single compact resonating unit cell element. A low cost thin FR4-epoxy dielectric is chosen to make the design economic. A simple dual split-ring geometry is used where the edges of the splits are bended inward to make the design compact and also increases coupling capacitance. A dual-band absorption is observed with this design because dual-mode resonances occur within the structure. The parametric studies on the design parameters G and L_0 show the effect of coupling on the absorption performance of the structure.

REFERENCES

1. Landy, N. I., S. Sajuyigbe, J. J. Mock, D. R. Smith, and W. J. Padilla, "Perfect metamaterial absorber," *Phys. Rev. Lett.*, Vol. 100, 207402, May 2008.
2. Ni, B., et al., "A dual-band polarization insensitive metamaterial absorber with split ring resonator," *Opt. Quant. Electron.*, Vol. 45, No. 7, 747–753, 2013.
3. Katsarakis, N., T. Koschny, and M. Kafesaki, "Electric coupling to the magnetic resonance of split ring resonators," *Appl. Phys. Lett.*, Vol. 84, No. 15, 2943–2945, 2004.
4. Gay-Balmaz, P. and O. J. Martin, "Electromagnetic resonances in individual and coupled split-ring resonators," *J. Appl. Phys.*, Vol. 92, No. 5, September 1, 2002.
5. Chaurasiya, D., S. Ghosh, S. Bhattacharyya, and K. V. Srivastava, "An ultrathin quad-band polarization-insensitive wide-angle metamaterial absorber," *Microwave Opt. Technol. Lett.*, Vol. 57, No. 2, 697–702, 2015.

6. Ghosh, S., S. Bhattacharyya, Y. Kaiprath, and K. Vaibhav Srivastava, "Bandwidth-enhanced polarization-insensitive microwave metamaterial absorber and its equivalent circuit model," *J. Appl. Phys.*, Vol. 115, 104503, 2014.

7. Sen, G., M. Kumar, S. N. Islam, and S. Das, "Design of a polarization insensitive absorptive frequency selective surface for radome applications," *2018 IEEE Indian Conference on Antennas and Propogation (InCAP)*, 1–3, Hyderabad, India, 2018.

8. Chejarla, S., S. R. Thummaluru, and R. K. Chaudhary, "Flexible metamaterial absorber with wide incident angle insensitivity for conformal applications," *Electronics Letters*, Vol. 55, No. 3, 133–134, February 7, 2019.

9. Ayop, O., M. K. A. Rahim, N. A. Murad, and N. A. Samsuri, "Dual resonance circular ring-shaped metamaterial absorber with wide operating angle," *2015 International Symposium on Antennas and Propagation (ISAP)*, 1–4, Hobart, TAS, 2015.

10. Zhai, H., C. Zhan, Z. Li, and C. Liang, "A triple-band ultrathin metamaterial absorber with wide-angle and polarization stability," *IEEE Antennas and Wireless Propagation Letters*, Vol. 14, 241–244, 2015.

11. Liu, Z., H. Zhang, S. Liu, B. Bian, and X. Kong, "An ultra-thin polarization-insensitive wide-angle metamaterial absorber," *2017 Progress In Electromagnetics Research Symposium — Spring (PIERS)*, 1887–1892, St Petersburg, Russia, May 22–25, 2017.

12. Sen, G. and S. Das, "Frequency tunable low cost microwave absorber for EMI/EMC application," *Progress In Electromagnetics Research Letters*, Vol. 74, 47–52, 2018.

13. Bayatpur, F. and K. Sarabandi, "Tuning performance of metamaterial-based frequency selective surfaces," *IEEE Transactions on Antennas and Propagation*, Vol. 57, No. 2, February 2009.

14. Li, L., Y. Yang, and C. H. Liang, "A wide-angle polarization-insensitive ultra-thin metamaterial absorber with three resonant modes," *J. Appl. Phys.*, Vol. 110, No. 6, 063702, 2011.

15. Zhong, J. P., et al., "Dual-band negative permittivity metamaterial based on cross circular loop resonator with shorting stubs," *IEEE Antennas and Wireless Propagation Letters*, Vol. 11, 803–806, 2012.

16. Kaur, K., T. Upadhyaya, and M. Palandoken, "Dual-band compact metamaterial-inspired absorber with wide incidence angle and polarization insensitivity for GSM and ISM band applications," *Radioengineering*, Vol. 27, 1025–1031, 2018, 10.13164/re.2018.1025.

17. Dincer, F., M. Karaaslan, E. Unal, K. Delihacioglu, and C. Sabah, "Design of polarization and incident angle insensitive dual-band metamaterial absorber based on isotropic resonators," *Progress In Electromagnetics Research*, Vol. 144, 123–132, 2014.

18. Zhai, H., Z. Li, L. Li, and C. Liang, "A dual-band wide-angle polarization-insensitive ultrathin gigahertz metamaterial absorber," *Microwave Opt. Technol. Lett.*, Vol. 55, 1606–1609, 2013.